International Journal of Computer Science and Information Technology
ISSN: 3005-9682 (Print), ISSN: 3005-7140 (Online) | Volume 3, Number 3, Year 2024
DOI: https://doi.org/10.62051/ijcsit.v3n3.04
Journal homepage: https://wepub.org/index.php/IJCSIT/index

Traffic Flow Prediction Based on VMD-ARO-BiLSTM

Haoxu Wang

College of Electrical and Information Engineering, Lanzhou University of Technology, Lanzhou, 730050, China

*Corresponding Author: 1099451942@qq.com

ABSTRACT

With the acceleration of urbanization and the continuous growth of transportation demand, traffic flow prediction has become a key research issue in ITS (Intelligent Transportation System). In this paper, a traffic flow prediction model based on VMD-ARO-BiLSTM is proposed, which can make full use of the spatio-temporal characteristics of traffic data to achieve high-precision traffic flow prediction. First, the traffic flow data are input into VMD (Variational Mode Decomposition) for data reconstruction. Then, the optimal parameter values of BiLSTM (Bi-directional Long Short-Term Memory) are solved using ARO (Artificial Rabbits Optimization) to complete the optimization of BiLSTM. Finally, the reconstructed data are input into BiLSTM to realize the accurate prediction of traffic flow. To verify the model performance, we conducted experiments using traffic flow data from different time periods. The experimental results show that on weekdays, the combined VMD-ARO-BiLSTM prediction model decreases the RMSE (Root Mean Square Error) by 47.2% and the MAE (Mean Absolute Error) by 44.6% compared to BiLSTM; on weekends, compared to BiLSTM, the RMSE decreases by 26.1% and MAE decreases by 23.4%, reflecting the strong robustness and applicability of this model, which has certain application value.

KEYWORDS

Traffic flow prediction; ARO; BiLSTM; VMD-ARO-BiLSTM combined prediction model

1. INTRODUCTION

There is an increasing imbalance between the supply and demand of urban roads, and with the rapid growth of automobile ownership, the problem of traffic congestion is becoming more and more prominent [1], which has seriously affected people's travel experience and quality of life. In order to effectively cope with these challenges, ITS has emerged, in which traffic flow prediction, as an important part of ITS, is of great significance to improve urban traffic efficiency, optimize route planning, and enhance the quality of travel services.

Traffic flow prediction is to collect and analyze traffic data to predict the traffic flow and traffic status in the future period. Accurate traffic flow prediction can help traffic management departments to formulate timely traffic management measures and guide drivers to choose appropriate travel routes, thus easing traffic congestion, reducing traffic accidents and decreasing environmental pollution. Therefore, traffic flow prediction has become one of the hotspots for scholars at home and abroad.

Raditional traffic flow prediction methods are mainly based on statistical and mathematical models, such as historical average models, time series models [2] and Kalman filter models [3]. These methods usually assume that the traffic flow follows a particular statistical distribution or law, and use historical data to predict the future traffic flow. However, these methods often suffer from high computational complexity and low prediction accuracy when dealing with large-scale and highdimensional traffic data. In addition, traditional methods are difficult to effectively capture the nonlinear relationships and spatio-temporal dependencies in traffic data, leading to inaccurate prediction results.

With the rapid development of computer technology, deep learning has received widespread attention and has achieved remarkable success in many fields, such as in image, audio and language learning tasks [4], providing new ideas for traffic flow prediction. Deep learning models have powerful feature extraction and learning capabilities, which can automatically extract useful information from raw data and construct complex functional relationships to describe the dependencies between data. Therefore, deep learning models have a broad application prospect in the field of traffic flow prediction.

Deep learning based traffic flow prediction models mainly include RNN (Recurrent Neural Network) and its variants [5-7]. RNN is a neural network model capable of processing sequence data, which treats each element in a sequence as an input by means of cyclic connectivity and utilizes internal hidden states to capture dependencies in the sequence. However, RNN are prone to the problem of gradient vanishing or gradient explosion when dealing with long sequences, leading to difficulties in model training. In order to solve this problem, LSTM (Long Short-Term Memory) is proposed and widely used in the field of traffic flow prediction. LSTM is based on RNN and adds a gating mechanism, which controls the flow of information through input gates, forgetting gates, and output gates, and thus effectively alleviates the problem of gradient vanishing and gradient explosion, and has a high prediction accuracy. Kang et al. [8] constructed a linear LSTM model for short-term traffic flow prediction by combining MSE (Mean Square Error) and Adam optimization algorithm. The experimental results show that the LSTM is able to capture the periodic characteristics of traffic flow with small error and high prediction accuracy. Mou et al. [9] proposed a T-LSTM model to improve the prediction accuracy by capturing the intrinsic correlation between the traffic flow and the time information. Experimental results show that this method can significantly improve the prediction performance.

Although LSTM have achieved remarkable results in the field of traffic flow prediction, in some cases, old information is gradually forgotten because the memory cells of LSTM are affected by forgetting gates when updating and cannot capture long-term dependencies effectively. To overcome this drawback, BiLSTM is gradually and widely used. BiLSTM consists of two LSTM networks, one dealing with forward time series data and the other dealing with reverse time series data, which enables BiLSTM to capture both forward and backward information in sequences, thus providing a more comprehensive understanding of sequence data. Ma et al. [10] established an LSTM and bi-directional LSTM network-based improved model, combining the advantages of sequence data and the long-term dependence of forward LSTM and backward LSTM, and integrating BiLSTM into the prediction model. The advantages of the proposed method in terms of accuracy and stability are demonstrated experimentally. Xing et al [11] constructed a fused data-driven DFBD-LSTM model for predicting single-lane and aggregated traffic flows by analyzing the spatio-temporal correlation of short-term traffic flows in multiple lanes. The model fused the characteristics of single-lane traffic flow and aggregated traffic flow to achieve more accurate prediction. Although all the above works achieved better prediction accuracy, the effects of traffic flow data and neural network hyperparameters on the prediction results were not considered.

Based on the above shortcomings, this paper proposes a traffic flow prediction method based on VMD-ARO-BiLSTM. Firstly, VMD is used to reconstruct the traffic flow data to remove the noise in the data; then ARO is used to optimize the hyperparameters of BiLSTM to give full play to the network performance. In this paper, a combined optimization prediction model is constructed to overcome the limitations of traditional methods and achieve efficient and accurate prediction of traffic flow.

2. METHODOLOGY

2.1. VMD

VMD is able to adaptively select the number of modal functions to be decomposed to apply to different types of signals according to the characteristics of the signals. It is well adapted to the time-frequency local structure of the signal, and can accurately separate the modal functions of different time scales in the data, overcoming the endpoint effect and the problem of modal component aliasing that exists in the EMD (Empirical Mode Decomposition) method, and avoiding the phenomenon of aliasing by controlling the bandwidth.

The VMD decomposition steps are as follows:

Step 1: Assume all modes $\{u_k\}=\{u_1,\cdots,u_K\}$ with center frequency $\{\omega_k\}=\{\omega_1,\cdots,\omega_K\}$, δ_t is the Dirac function, f is the original signal, α is the regularization parameter representing the variance of the white noise, λ is the Lagrangian algorithm factor, and $\hat{f}(\omega),\hat{u}_i(\omega),\hat{\lambda}^n(\omega)$ are the Fourier transform of $f(t),u_i(t),\lambda^n(t)$, respectively.

Step 2: The original minimization problem in Eq. (1) becomes the problem of solving the saddle point in Eq. (2).

$$\begin{cases} \min\limits_{\{u_k\},\{\omega_k\}} \left\{ \sum_k \left\| \partial_t \left[\left(\delta(t) + \frac{j}{\pi t} \right) u_k(t) \right] e^{-j\omega_k t} \right\|_2^2 \right\} \\ \text{s.t.} \sum_k u_k = f \end{cases} \tag{1}$$

$$\begin{aligned} L(\{u_k\},\{\omega_k\},\lambda) = \alpha \sum_k \left\| \partial_t \left[\left(\delta(t) + \frac{j}{\pi t} \right) u_k(t) \right] e^{-j\omega_k t} \right\|_2^2 + \\ \left\| f(t) - \sum_k u_k(t) \right\|_2^2 + \left\langle \lambda(t), f(t) - \sum_k u_k(t) \right\rangle \end{aligned} \tag{2}$$

Step 3: The modal components and center frequency are updated with ADMM (Alternating Direction Multipliers) and finally the saddle point is obtained.

Step 4: Initialization $\{\hat{u}_k^1\},\{\boldsymbol{\omega}_k^1\},\hat{\lambda}^1,n\leftarrow 0$.

Step 5: Enter the loop $n\leftarrow n+1$.

Step 6: Update ω_k; if $\omega\geqslant 0$, then update $\hat{u}_k$.

$$\hat{u}_k^{n+1}(\omega) \leftarrow \frac{\hat{f}(\omega) - \sum_{i<k} \hat{u}_i^{n+1}(\omega) - \sum_{i>k} \hat{u}_i^n(\omega) + \frac{\hat{\lambda}^n(\omega)}{2}}{1 + 2\alpha(\omega - \omega_k^n)^2} \tag{3}$$

$$\omega_k^{n+1} \leftarrow \frac{\int_0^\infty \omega |\hat{u}_k^{n+1}(\omega)|^2 \mathrm{d}\omega}{\int_0^\infty |\hat{u}_k^{n+1}(\omega)|^2 \mathrm{d}\omega} \tag{4}$$

Step 7: Update $\hat{\lambda}$ by double rising for all terms with $\omega\geqslant 0$.

$$\hat{\lambda}^{n+1}(\omega) \leftarrow \hat{\lambda}^n(\omega) + \tau \left(\hat{f}(\omega) - \sum_k \hat{u}_k^{n+1}(\omega) \right) \tag{5}$$

Step 8: Determine whether $\sum_k \|\hat{u}_k^{n+1} - \hat{u}_k^n\|_2^2 / \|\hat{u}_k^n\|_2^2 < \varepsilon$ is satisfied. If satisfied, output ω_k and $\hat{u}_k$, otherwise return to step five.

By finding the optimal solution of the constrained variational model, VMD decomposes the nonsmooth traffic flow time series into various modal components, reduces the nonsmoothness of the time series, and decomposes the time series to obtain the sub-series that contains several different frequency scales and is relatively smooth.

2.2. ARO

The ARO algorithm [12], as a new optimization algorithm, references two behaviors of rabbits: meandering foraging and random hiding. In this case, meandering foraging as an exploratory strategy is used to prevent the rabbit from being detected by predators by having it eat grass near the nest. Random hiding is when the rabbit moves to other burrows in order to hide further away. Initialization is done as follows:

$$\vec{z}_{i,k} = r \cdot (ub_k - lb_k) + lb_k, k = 1, 2, \cdots, d \tag{6}$$

Where $\vec{z}_{i,k}$ denotes the position of the jth dimension of the ith rabbit, r is the random number given along with it, d is the number of variable dimensions, N is the size of the artificial rabbit population, ub and lb are upper and lower bounds.

Meandering foraging involves each rabbit churning around the food source and exploring a randomly selected location of another rabbit in the group to obtain enough food. The updated formula for meandering foraging is shown in Eq:

$$\vec{v}_i(t+1) = \vec{z}_j(t) + R \cdot (\vec{z}_i(t) - \vec{z}_j(t)) + round(0.5 \cdot (0.05 + r_1)) \cdot n_1 \tag{7}$$

In Eq. (7), t indicates the present iteration count. $\vec{v}_i(t+1)$ represents the new placement of the ith artificial rabbit. $\vec{z}_i(t)$ and $\vec{z}_j(t)$ denote the ith and other randomly located artificial rabbits, $i,j = 1,...,N$, N is the size of the rabbit population. R stands for the run operator. $round$ signifies rounding to the closest whole number. r_1 is three random numbers of $(0,1)$.

Random hiding is modeled after the exploration phase of the algorithm. Rabbits usually dig several holes around their nests and then randomly choose one to hide in order to reduce the probability of predation. The updated formula for the random hiding strategy is shown below.

$$\vec{v}_i(t+1) = \vec{z}_i(t) + R \cdot \left(r_4 \cdot \vec{b}_{i,r}(t) - \vec{z}_i(t)\right), \tag{8}$$

Where $\vec{b}_{i,r}(t)$ denotes a randomly selected burrow among d burrows generated by the rabbit to hide. r_4 denotes a random numbers of $(0,1)$.

After implementing the two update strategies, the position of the first artificial rabbit is updated by Eq. (9).

$$\vec{z}_i(t+1) = \begin{cases} \vec{z}_i(t) & f(\vec{z}_i(t)) \leq f(\vec{v}_i(t+1)) \\ \vec{v}_i(t+1) & f(\vec{z}_i(t)) > f(\vec{v}_i(t+1)) \end{cases} \tag{9}$$

In Eq. (9), where f is the adaptation value, the formula indicates that the rabbit autonomously decides whether to remain at its current position or relocate to a new position based on the adaptation value.

2.3. BiLSTM

LSTM is a special RNN architecture that solves the problems of gradient vanishing and gradient explosion that exist in traditional RNN when dealing with long sequence data. By introducing a gating mechanism, LSTM is able to capture and memorize long-term dependencies. LSTM consists of forgetting gates, input gates and output gates, and the structure is shown in Fig. 1.

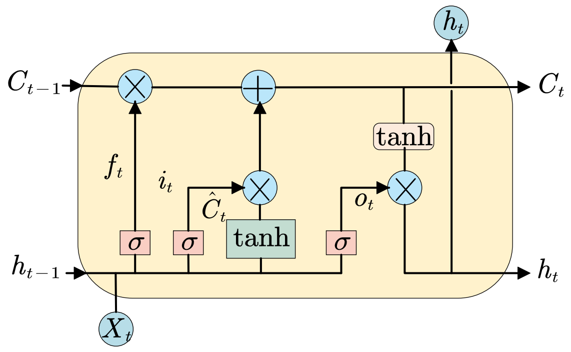

Figure 1. LSTM model structure

The information transfer process within LSTM is shown below:

$$i_t = \sigma(W_i x_t + U_i h_{t-1} + b_i) \tag{10}$$

$$f_t = \sigma(W_f x_t + U_f h_{t-1} + b_f) \tag{11}$$

$$\hat{C}_t = \tanh(W_c x_t + U_c h_{t-1} + b_c) \tag{12}$$

$$C_t = f_t \odot C_{t-1} + i_t \odot \hat{C}_t \tag{13}$$

$$o_t = \sigma(W_o x_t + U_o h_{t-1} + b_o) \tag{14}$$

$$h_t = o_t \odot \tanh(C_t) \tag{15}$$

Where x_t is the input sequence at time t; i_t, f_t, o_t are the output of the input gate, forgetting gate and output gate respectively, which are used to control the path of information transmission; $W_i, W_f, W_c, W_o, U_i, U_f, U_c, U_o$ are the corresponding weight matrix; b_i, b_f, b_c, b_o are the corresponding bias term; h_{t-1} and h_t are the output values of the hidden layer at times $t-1$ and t respectively; C_{t-1} and C_t are the memory cell states at times $t-1$ and t; $\hat{C}_t$ is the new candidate state; σ is the sigmoid activation function; $\tanh$ is the hyperbolic tangent function.

The traffic flow sequence has strong temporal characteristics, and the traffic flow changes at the current moment are not only related to the information of the past moment, but also related to the information of the future moment. Therefore, an LSTM that conveys information in reverse time order is added to the forward LSTM to form BiLSTM. The hidden layer states of the forward LSTM and the backward LSTM are spliced at each time step to produce the final hidden layer state at that time step. This combination allows the BiLSTM to take into account both past and future temporal information, thus improving the prediction of traffic flow sequence data. The BiLSTM structure is shown in Fig. 2.

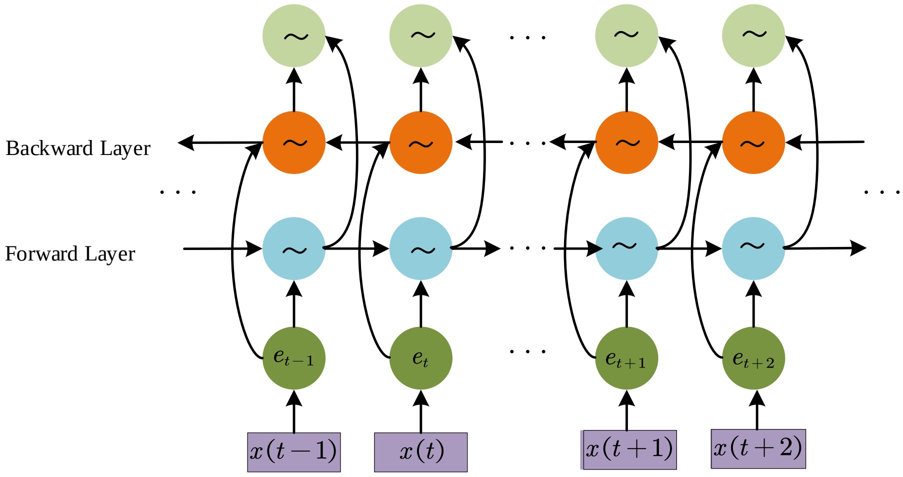

Figure 2. BiLSTM model structure

3. VMD-ARO-BILSTM TRAFFIC FLOW PREDICTION MODEL

In this paper, the traffic flow data is first divided into training set and test set in 7:3, and then the data is decomposed and noise reduction using VMD to get the input data for the prediction model. The prediction model integrates the ARO algorithm on the basis of BiLSTM, and calculates the fitness value of ARO for each iteration in an iterative way, so as to find the optimal number of hidden units and the learning rate of BiLSTM, and give full play to the prediction performance of BiLSTM. The model framework of VMD-ARO-BiLSTM is shown in Fig. 3.

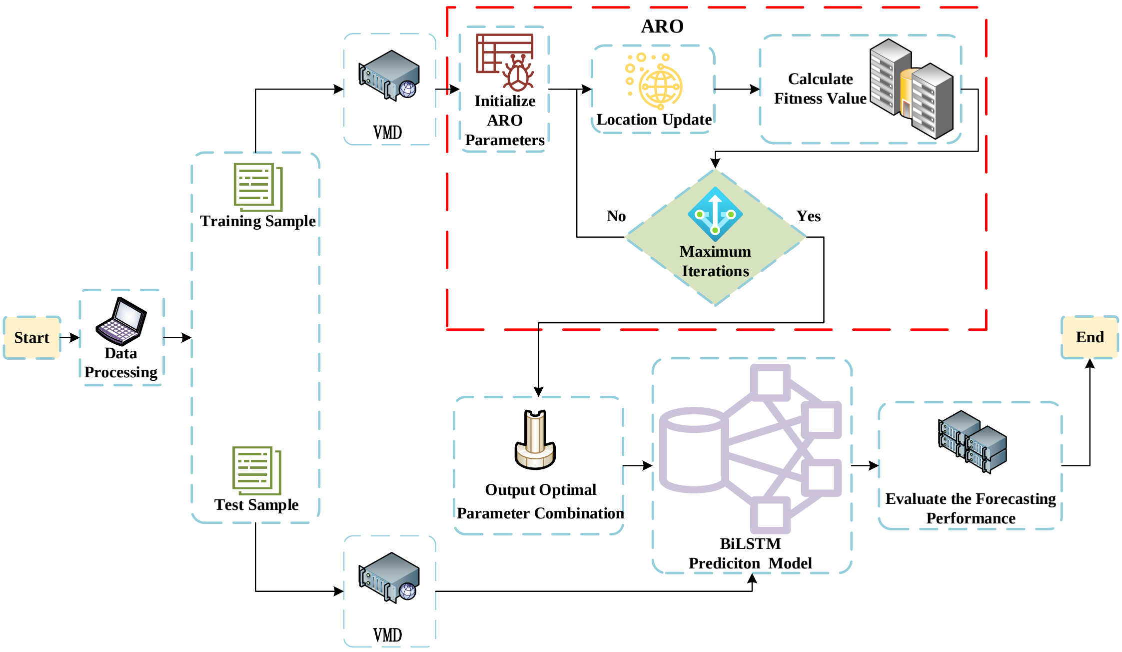

Figure 3. VMD-ARO-BiLSTM modeling framework

4. EXPERIMENTAL ANALYSIS

4.1. Evaluation Indicators

The experimental data in this paper adopts the UK highway public dataset as the data source, and selects R^2, MAE and RMSE as the evaluation indexes to compare the performance of the prediction model with the following formulas.

$$R^2 = 1 - \frac{\sum_{i=0}^{n_{samples}-1} (y^* - y)^2}{\sum_{i=0}^{n_{samples}-1} (y - \bar{y})} \tag{16}$$

$$\mathrm{MAE} = \frac{1}{n}\sum_{i=1}^{n} |y^* - y| \tag{17}$$

$$\mathrm{RMSE} = \sqrt{\frac{1}{n}\sum_{i=1}^{n} (y^* - y)^2} \tag{18}$$

In Eq. (16)-(18),n is the sample size,y^* is the predicted value,y is the actual value. The smaller the values of RMSE and MAE, the larger the values of R^2, the higher the accuracy of the model.

4.2. Model Analysis

In this paper, the number of populations of ARO is set to 20, the number of iterations is set to 50, the neural network optimizer is the Adam optimizer, the loss function is MSE, the epoch is set to 100, and the input is one hour of traffic flow data.

In order to verify the prediction effect of the proposed combined prediction model in different scenarios, this paper analyzes the prediction of traffic flow on weekdays and weekends respectively.

Fig. 4 and Fig. 5 show the prediction effects of VMD-ARO-BiLSTM for weekend and weekday traffic flows, respectively. Tab. 1 and Tab. 2 show the prediction results, respectively. It can be seen that the prediction results of each prediction model for weekday and weekend traffic flow are significantly different, which is due to the different traffic patterns on weekdays and weekends. On weekdays, vehicles have a relatively fixed commuting time, and the traffic flow fluctuates a lot, which makes it difficult for the model to capture the features of the data, and the prediction accuracy is relatively low; on weekends, the commuting time of the vehicles is more dispersed, and the traffic flow is reduced compared to weekdays, which is easier for the model to capture the traffic flow features, and the prediction accuracy is relatively high.

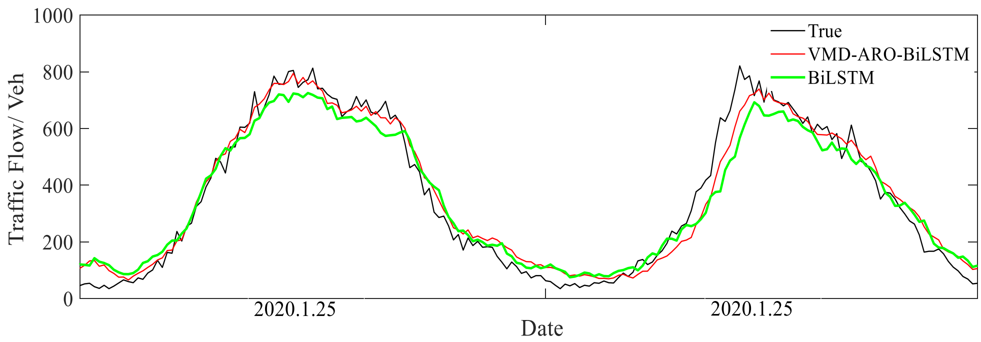

Figure 4. Effect of weekend prediction

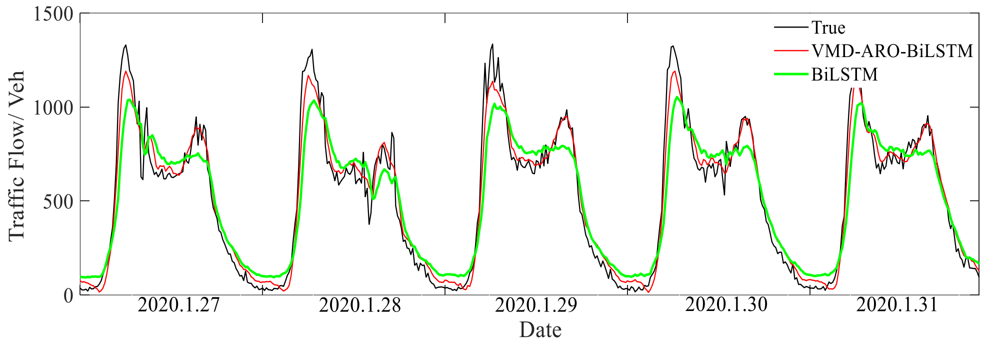

Figure 5. Effectiveness of workday forecasting

Compared with the BiLSTM model, the combined VMD-ARO-BiLSTM prediction model proposed in this paper substantially improves the prediction accuracy at different time periods. On weekdays, the RMSE of VMD-ARO-BiLSTM model decreases by 47.2% and MAE decreases by 44.6% compared with BiLSTM; on weekends, the RMSE of VMD-ARO-BiLSTM model decreases by 26.1% and MAE decreases by 23.4% compared with BiLSTM, which reflects that the present model has a strong robustness and generalization ability.

Table 1. Weekend forecast results

Model	RMSE	MAE	R^2
BiLSTM	64.5293	49.6023	0.93494
ARO-BiLSTM	52.3197	37.4731	0.95723
VMD-ARO-BiLSTM	47.6651	37.9745	0.96451

Table 2. Results of working day projections

Model	RMSE	MAE	R^2
BiLSTM	135.3369	98.258	0.86968
ARO-BiLSTM	98.9826	70.3756	0.93029
VMD-ARO-BiLSTM	71.4422	54.461	0.96368

5. CONCLUSION

In this paper, a traffic flow prediction model based on VMD-ARO-BiLSTM is proposed to accurately predict traffic flow, which effectively captures the spatio-temporal characteristics of traffic flow data. The experimental results show that the model achieves excellent prediction performance on traffic flow datasets of different time periods, and the prediction performance is substantially improved compared with BiLSTM.

The VMD-ARO-BiLSTM model proposed in this paper shows excellent accuracy and generalization ability in the traffic flow prediction task, which can effectively capture the rapid changes of traffic flow, demonstrates good robustness, provides valuable decision-making suggestions for traffic managers, and has high feasibility in practical applications.

REFERENCES

[1] W. B. Zhang, H. Z. Zha, S. Zhang, and L. Ma, "Road section traffic flow prediction method based on the traffic factor state network," Physica a-Statistical Mechanics and Its Applications, vol. 618, pp. 18, May, 2023.

[2] S. V. Kumar, and L. Vanajakshi, "Short-term traffic flow prediction using seasonal ARIMA model with limited input data," European Transport Research Review, vol. 7, no. 3, pp. 9, Sep, 2015.

[3] S. V. Kumar, "Traffic Flow Prediction using Kalman Filtering Technique," Procedia Engineering. pp. 582-587, 2017.

[4] Q. X. Lieu, “A deep neural network-assisted metamodel for damage detection of trusses using incomplete time-series acceleration,” Expert Systems with Applications, vol. 233, pp. 120967, 2023.

[5] W. Fitters, A. Cuzzocrea, and M. Hassani, "Enhancing LSTM Prediction of Vehicle Traffic Flow Data via Outlier Correlations," Proceedings International Computer Software and Applications Conference. pp. 210-217, 2021.

[6] W. Y. Wei, H. H. Wu, and H. Ma, “An AutoEncoder and LSTM-Based Traffic Flow Prediction Method,” Sensors, vol. 19, no. 13, pp. 16, Jul, 2019.

[7] Z. Y. Li, H. X. Ge, and R. J. Cheng, “Traffic flow prediction based on BILSTM model and data denoising scheme,” Chinese Physics B, vol. 31, no. 4, pp. 10, Mar, 2022.

[8] C. L. Kang, Z. Y. Zhang, and Ieee, "Application of LSTM in Short-term Traffic Flow Prediction." pp. 98-101, 2020.

[9] L. T. Mou, P. F. Zhao, H. T. Xie, and Y. Y. Chen, “T-LSTM: A Long Short-Term Memory Neural Network Enhanced by Temporal Information for Traffic Flow Prediction,” Ieee Access, vol. 7, pp. 98053-98060, 2019.

[10] C. X. Ma, G. W. Dai, and J. B. A. Zhou, “Short-Term Traffic Flow Prediction for Urban Road Sections Based on Time Series Analysis and LSTM_BILSTM Method,” Ieee Transactions on Intelligent Transportation Systems, vol. 23, no. 6, pp. 5615-5624, Jun, 2022.

[11] L. M. Xing, and W. J. Liu, “A Data Fusion Powered Bi-Directional Long Short Term Memory Model for Predicting Multi-Lane Short Term Traffic Flow,” Ieee Transactions on Intelligent Transportation Systems, vol. 23, no. 9, pp. 16810-16819, Sep, 2022.

[12] L. Y. Wang, Q. J. Cao, Z. X. Zhang, S. Mirjalili, and W. G. Zhao, “Artificial rabbits optimization: A new bio-inspired meta-heuristic algorithm for solving engineering optimization problems,” Engineering Applications of Artificial Intelligence, vol. 114, pp. 31, Sep, 2022.